LA-UR-18-31171
Approved for public release; distribution is unlimited.

Title: Electron Environment at Geostationary Orbit: AE9 Summary Results

Author(s): Larsen, Brian Arthur

Intended for: Report

Issued: 2018-11-29

Disclaimer:
Los Alamos National Laboratory, an affirmative action/equal opportunity employer, is operated by Triad National Security, LLC for the National Nuclear Security Administration of U.S. Department of Energy under contract 89233218CNA000001. By approving this article, the publisher recognizes that the U.S. Government retains nonexclusive, royalty-free license to publish or reproduce the published form of this contribution, or to allow others to do so, for U.S. Government purposes. Los Alamos National Laboratory requests that the publisher identify this article as work performed under the auspices of the U.S. Department of Energy. Los Alamos National Laboratory strongly supports academic freedom and a researcher's right to publish; as an institution, however, the Laboratory does not endorse the viewpoint of a publication or guarantee its technical correctness.

Electron Environment at Geostationary Orbit: AE9 Summary Results

B. A. Larsen

November 28th, 2018

Space Science and Applications
Los Alamos National Laboratory
P.O. Box 1663
Los Alamos, NM, 87545 USA

Table of Contents

1. *Introduction* 3
2. *Model and Setup* 3
3. *Overview* 4
4. *Results and Narrative* 5
5. *Other Resources* 10
6. *References* 10
7. *Appendix: Tabulated Spectra* 11

1. Introduction

This report captures the outputs from the AE9 for the electron environment at geostationary orbit. There is no new work, simply a collection of model outputs to make them easier to use and tailored to quick data gathering for geostationary orbit studies. Other models do exist, such as POLE [1], but a comprehensive look at each is beyond the scope of this work. Other resources are contained in the references.

2. Model and Setup

The model utilized is the AE9 model version 1.50.001 [2-5]. AE9/AP9 is the new community standard trapped radiation specification model following after the AE8/AP8 model [6]. For this work, the model was run on OSX through wine [7] and analyzed using the ae9ap9 module in SpacePy [8], pandas [9], matplotlib [10], jupyter notebooks [11], and SciPy [12], all in python 3.7 [13]. The model parameters are shown in Figure 1. The variation as a function of time was found to be minimal after a yearly run with 60 second resolution so one day was run for all the cases. Ephemeris was computed in geocentric equatorial inertial (GEI) coordinates [14] and reported fluxes are omnidirectional and differential in energy. In GEI coordinates geostationary orbit forms a circle at 6.6 Earth radii (Re) as shown in Figure 2. Identical model runs were performed for longitudes every 20 degrees around the globe. Percentile fluxes every 5% from 5% to 95% were tabulated. For the AE9 model percentiles are the fraction of the data below a given flux value over all time. This intentionally does not have a solar cycle or other dependence in order to give these percentiles the intended meaning.

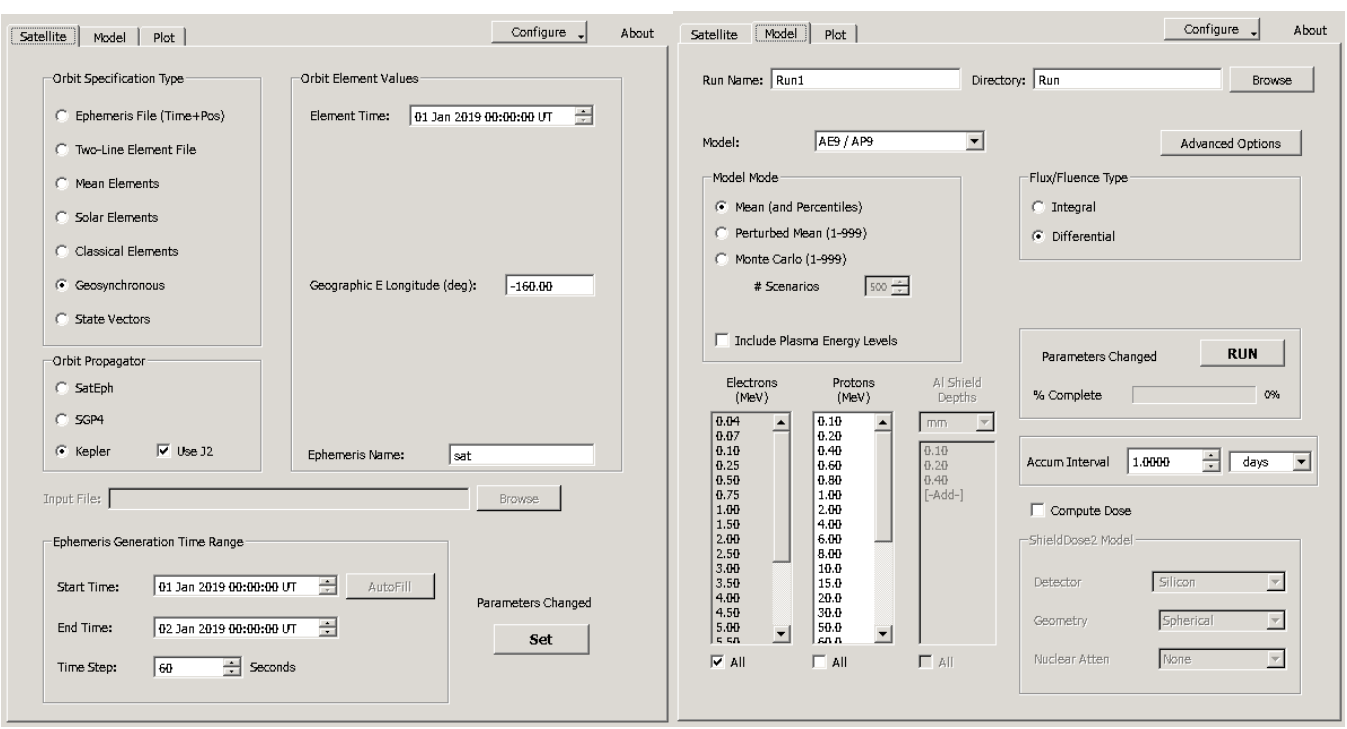

Figure 1 Screenshots of the AE9 model parameters.

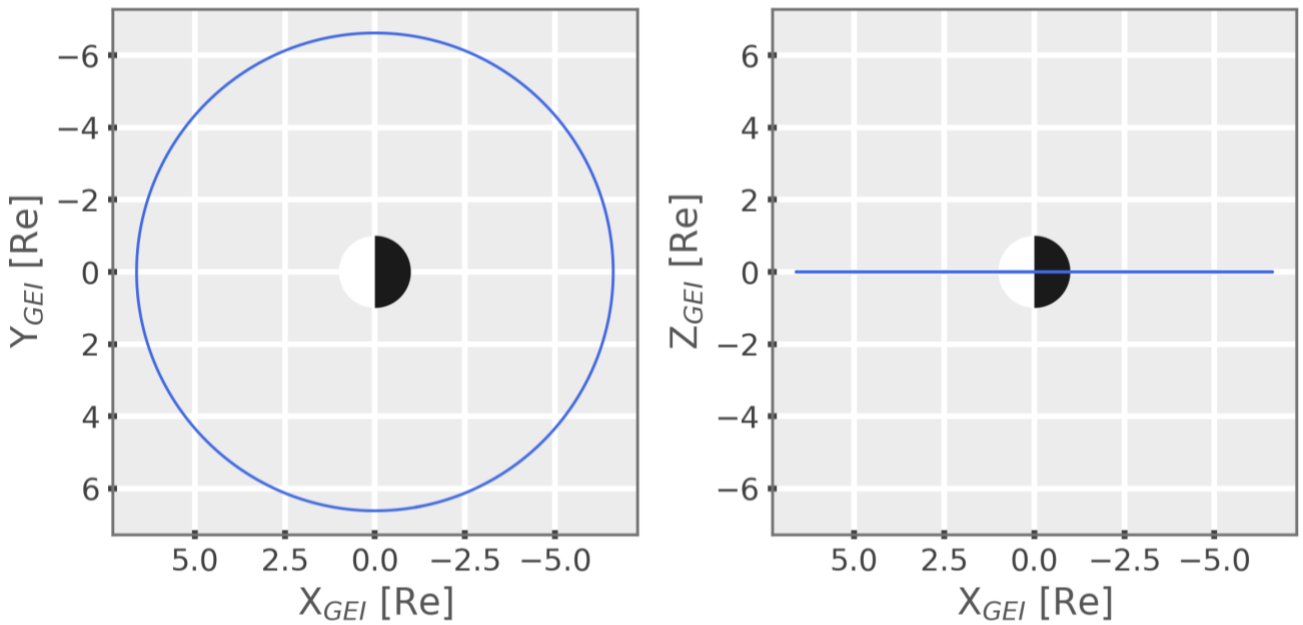

Figure 2 Plot of a one-day orbit track in geostationary orbit in GEI coordinates.

3. Overview

The energetic (~MeV) trapped electron population is known as the Van Allen Radiation belt [15]. These electrons are trapped on magnetic field lines and the magnetic field is not aligned with Earth's spin axis. Figure 3 shows a schematic view of Earth's magnetosphere. The trapped electron population is in the Co-rotation region noted in the figure.

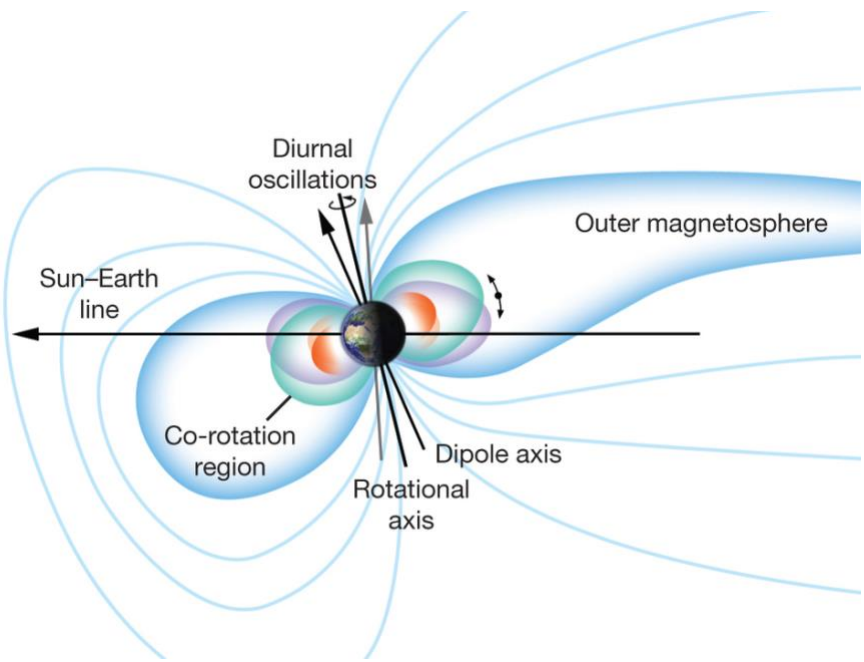

Figure 3 Schematic view of Earth's magnetosphere, from [16].

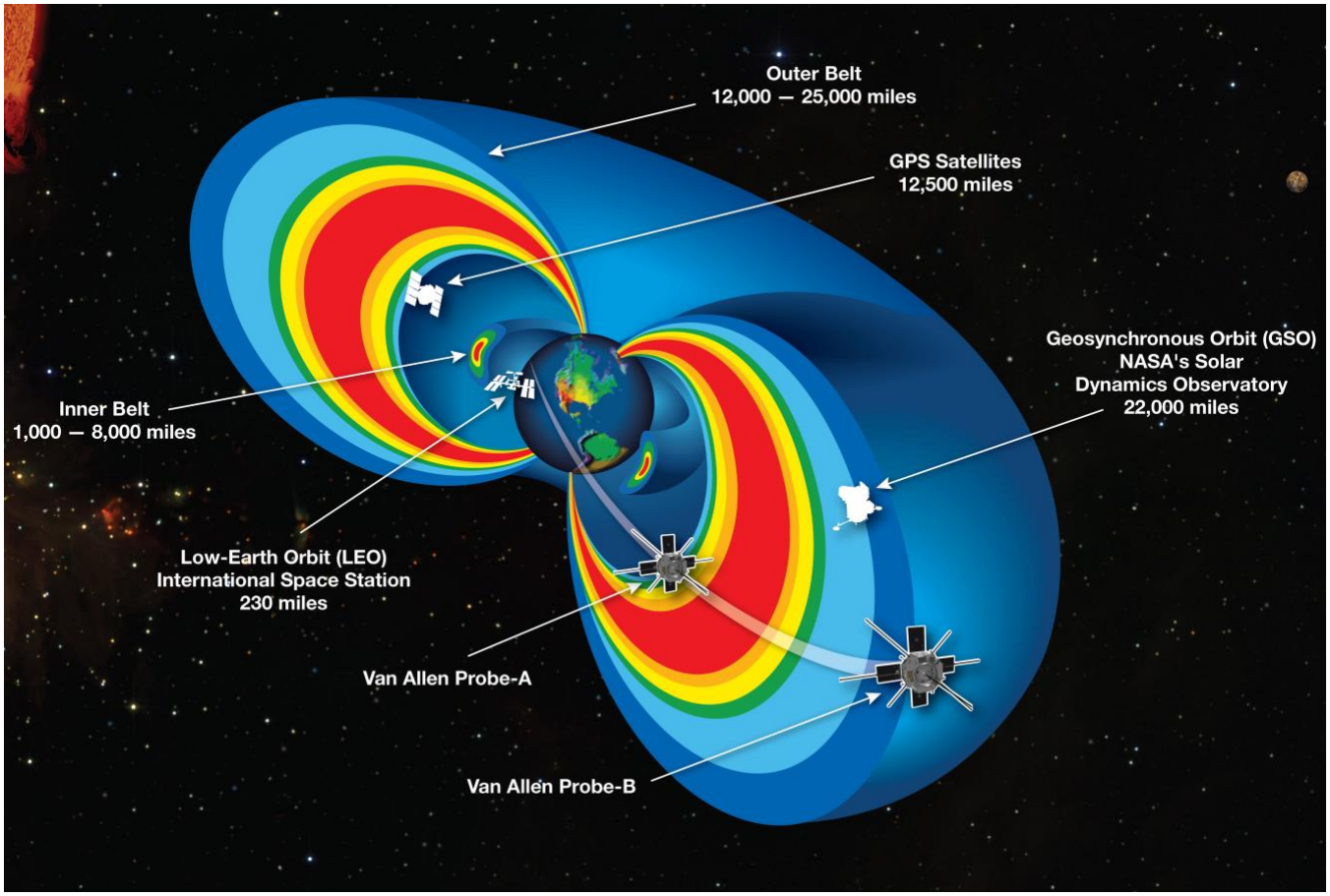

Figure 4 Figure showing the notional radiation belt intensity as a function of location around the Earth. Several orbits are denoted with their position relative to the notional maximum. From NASA.

4. Results and Narrative

This section contains model output results and a narrative on how to utilize these outputs for follow-on studies.

The electron radiation belt has a huge variation in intensity, Figure 5 shows the difference with energy and with percentile. For the same energy, 1 MeV as an example, there is a factor of 489 between 95th and 5th percentile. Figure 6 shows the ratios between 95th/5th and 95th/50th as a function of energy for 0° longitude.

The electron radiation belt has a strong energy dependence. Figure 9 shows the energy spectra as a function of percentile. In the AE9 model there is little dependence on percentile for the spectral shape.

The electron radiation belt has a slight dependence on longitude. Figure 10 shows the ratio compared to 0° longitude for several energies and percentiles.

As the fluxes as a very steep function of energy and percentile, special care must be taken in interpolation. Good choices are BSpline and Piecewise Cubic Hermite Interpolating Polynomial (PCHIP) both part of scipy interpolate.

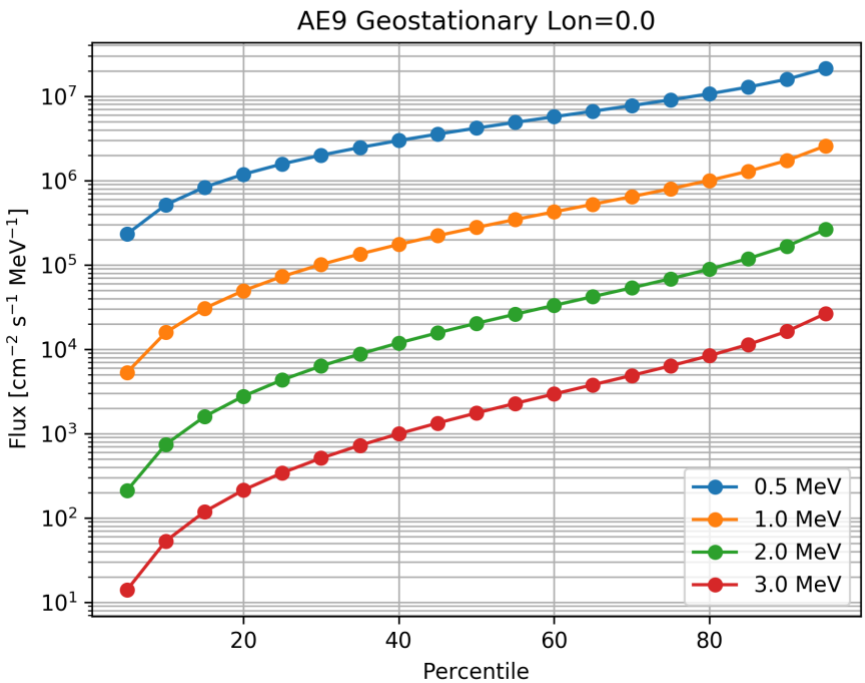

Figure 5 Radiation belt fluxes are a falling spectrum with roughly an order of magnitude between each of the presented energies.

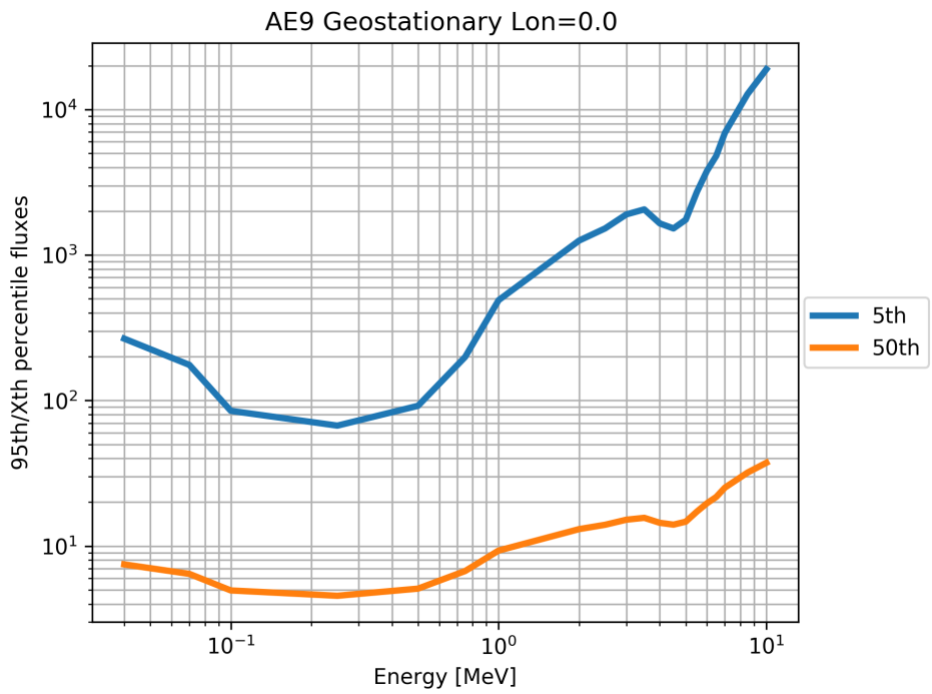

Figure 6 Flux ratios between 95th and 5th and 50th percentiles for 0° longitude.

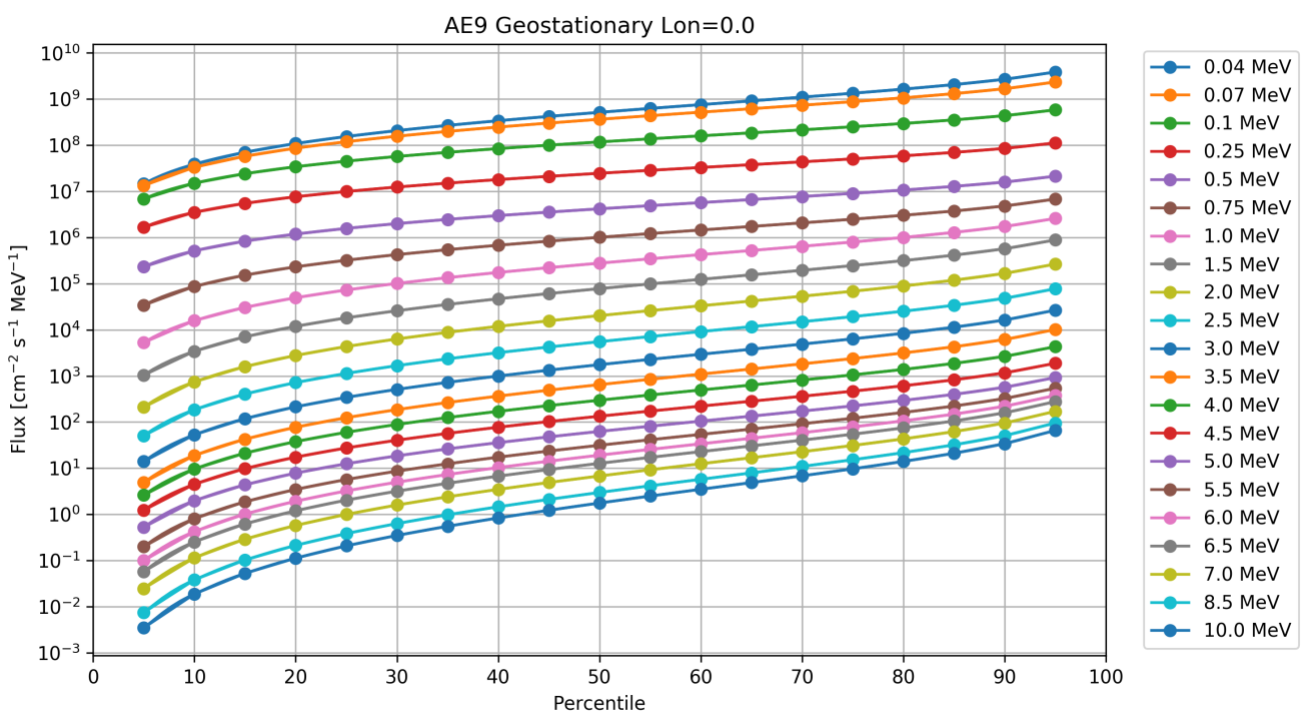

Figure 7 All computed fluxes and a function of percentile at 0° longitude.

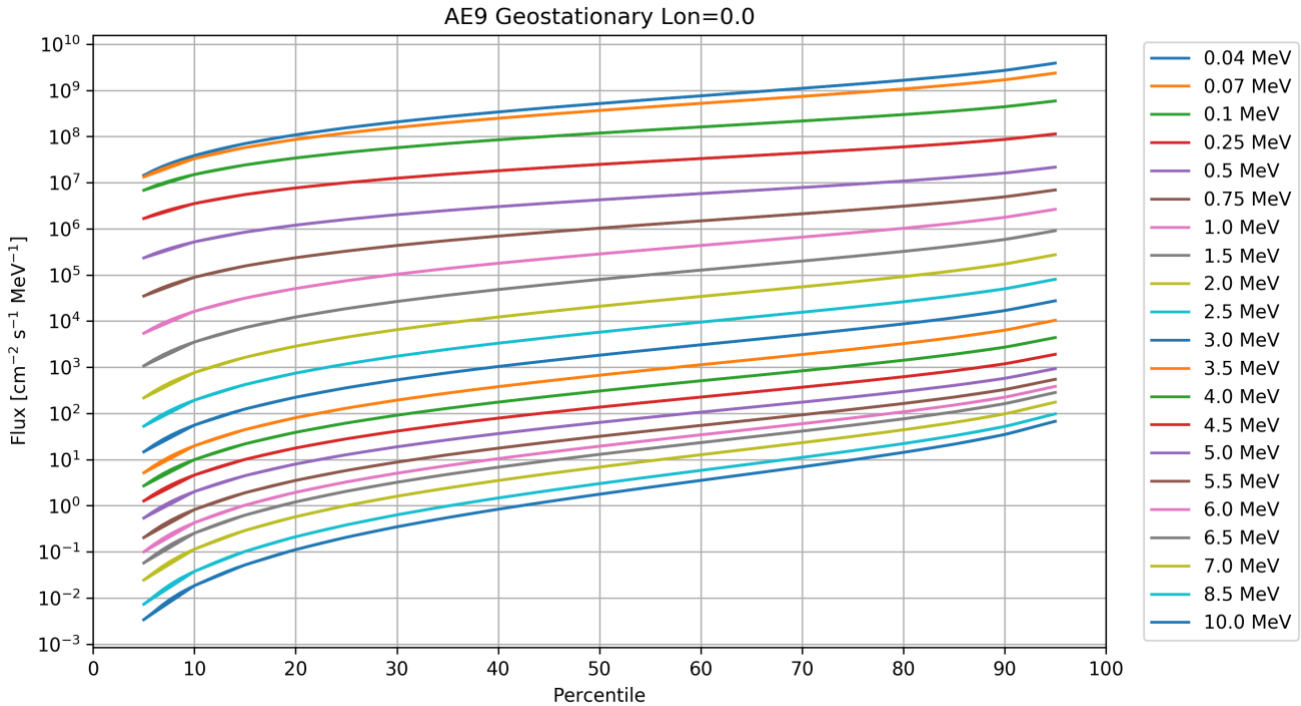

Figure 8 All computed fluxes and a function of percentile at 0° longitude. This is the same as Figure 7 without the points drawn.

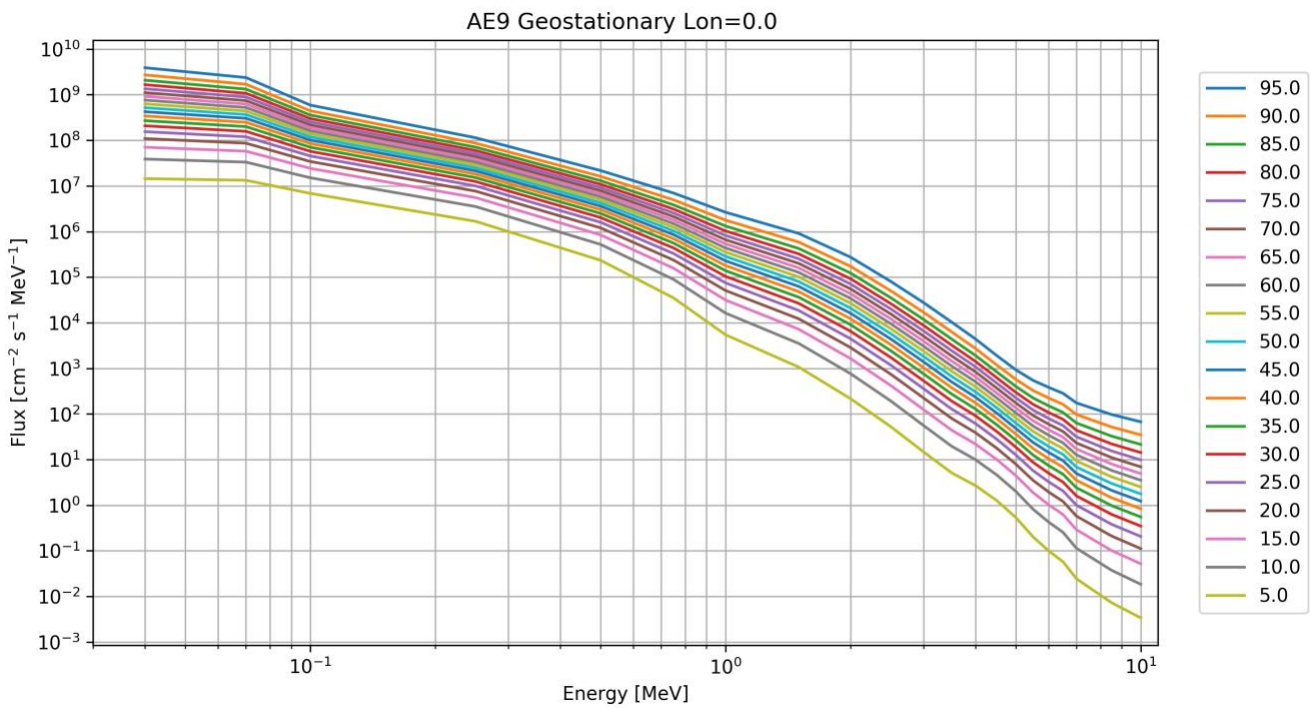

Figure 9 All computed fluxes as a function of energy for various percentiles at 0° longitude.

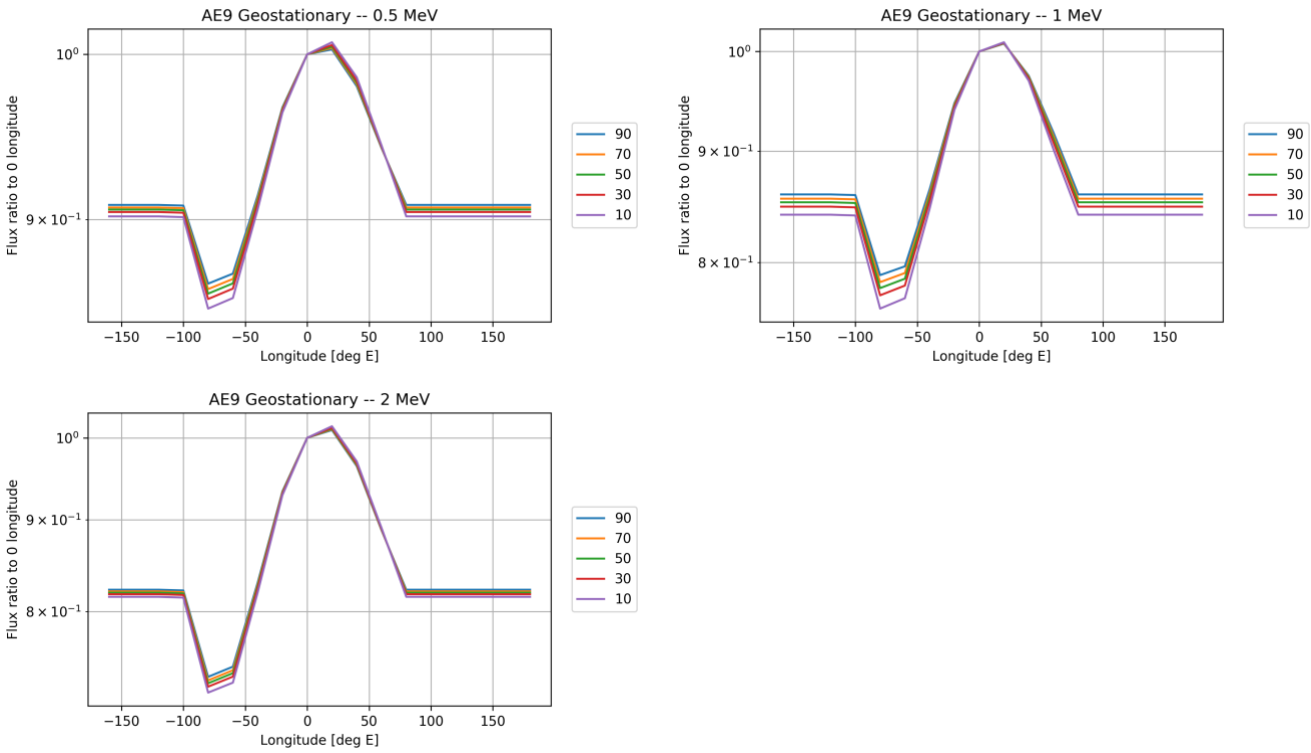

Figure 10 Flux ratios as a function of longitude and percentile compared to the value at 0°.

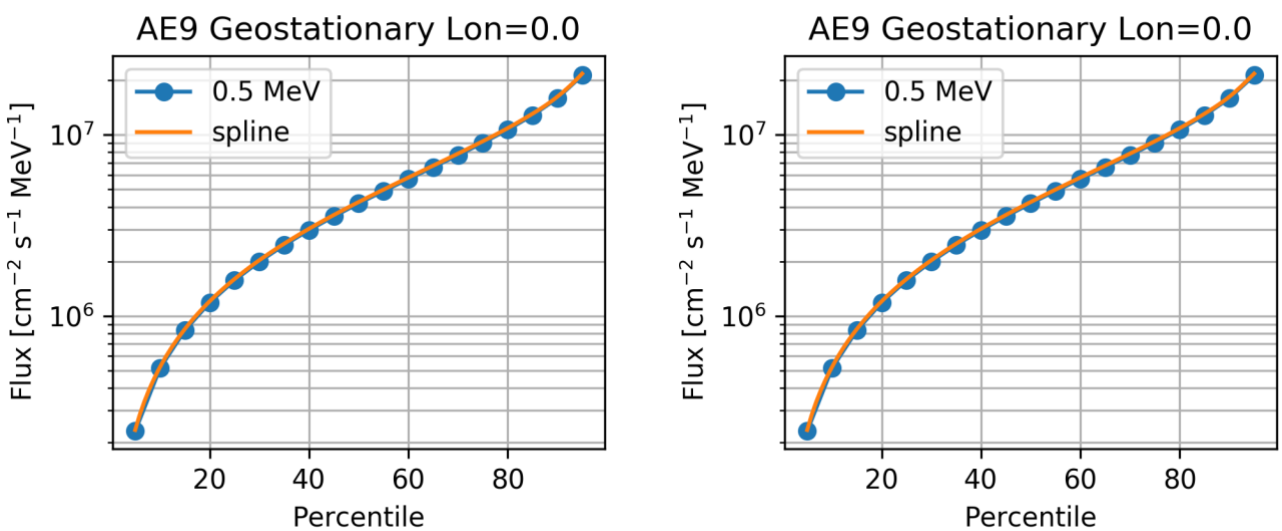

Figure 11 Example interpolations in percentile space, left is BSpline and right is PCHIP.

5. Other Resources

Textbooks: [14, 17-19]

Presentations: [20]

This work, code, and data are cataloged for LANL use at: https://git.lanl.gov/SABRS-NGP/geo-swx-percentiles

6. References

1. Boscher, D., et al., *Model for the geostationary electron environment: POLE.* IEEE Transactions on Nuclear Science, 2003. **50**(6): p. 2278-2283.
2. Ginet, G., et al., *AE9, AP9 and SPM: New models for specifying the trapped energetic particle and space plasma environment*, in *The Van Allen Probes Mission*. 2013, Springer. p. 579-615.
3. Johnston, W.R., et al. *AE9/AP9/SPM: New models for radiation belt and space plasma specification*. in *Sensors and Systems for Space Applications VII*. 2014. International Society for Optics and Photonics.
4. Johnston, W.R., et al., *Recent updates to the AE9/AP9/SPM radiation belt and space plasma specification model.* IEEE Transactions on Nuclear Science, 2015. **62**(6): p. 2760-2766.
5. Roth, C., *AE9/AP9/SPM radiation environment model: User's guide*. 2014, ATMOSPHERIC AND ENVIRONMENTAL RESEARCH INC LEXINGTON MA.
6. Bilitza, D., *Models of trapped particle fluxes AE8 (electrons) and AP8 (protons) in inner and outer radiation belts.* NSSDC Code, 1987. **633**.
7. Amstadt, B. and M.K. Johnson, *Wine.* Linux Journal, 1994. **1994**(4es): p. 3.
8. Morley, S.K., et al. *SpacePy—a python-based library of tools for the space sciences*. in *Proceedings of the 9th Python in science conference (SciPy 2010)*. 2010.
9. McKinney, W. *Data structures for statistical computing in python*. in *Proceedings of the 9th Python in Science Conference*. 2010. Austin, TX.
10. Hunter, J.D., *Matplotlib: A 2D graphics environment.* Computing in science & engineering, 2007. **9**(3): p. 90-95.
11. Kluyver, T., et al. *Jupyter Notebooks-a publishing format for reproducible computational workflows*. in *ELPUB*. 2016.
12. Jones, E., T. Oliphant, and P. Peterson, *{SciPy}: open source scientific tools for {Python}.* 2014.
13. Rossum, G., *Python reference manual.* 1995.
14. Kivelson, M. and C. Russell, *Introduction to Space Physics, Cambridge atmospheric and space science series*. 1995, Cambridge University Press.
15. Van Allen, J.A. and L.A. Frank, *Radiation around the Earth to a radial distance of 107,400 km.* Nature, 1959. **183**.
16. Ukhorskiy, A., et al., *Rotationally driven 'zebra stripes' in Earth's inner radiation belt.* Nature, 2014. **507**(7492): p. 338.
17. Parks, G., *Physics of space plasmas: an introduction (Boulder, CO*. 2004, Westview Press.
18. Moldwin, M., *An introduction to space weather*. 2008: Cambridge University Press.
19. Bothmer, V. and I.A. Daglis, *Space weather: physics and effects*. 2007: Springer Science & Business Media.

20. Larsen, B.A., *Heliophysics in the SNDD Context*. 2017, Los Alamos National Lab.(LANL), Los Alamos, NM (United States).

7. Appendix: Tabulated Spectra

This appendix contains tabulated spectra for 0° longitude. Column header are percentile fluxes, the rows are energies (MeV), and the values of the omnidirectional differential electron number flux ($cm^{-2}s^{-1}MeV^{-1}$).

	95	90	85	80	75	70	65	60	55	50	45	40	35	30	25	20	15	10	5
0.04	3.85E+09	2.68E+09	2.05E+09	1.64E+09	1.34E+09	1.1E+09	9.11E+08	7.56E+08	6.26E+08	5.15E+08	4.21E+08	3.39E+08	2.68E+08	2.07E+08	1.54E+08	1.09E+08	70385059	38842932	14478536
0.07	2.34E+09	1.67E+09	1.31E+09	1.06E+09	8.78E+08	7.34E+08	6.17E+08	5.19E+08	4.36E+08	3.64E+08	3.01E+08	2.47E+08	1.99E+08	1.56E+08	1.19E+08	86176173	57610569	33225158	13323047
0.1	5.82E+08	4.37E+08	3.53E+08	2.95E+08	2.51E+08	2.15E+08	1.85E+08	1.6E+08	1.37E+08	1.18E+08	1E+08	84295341	69980799	56945051	45032124	34125115	24142577	15043587	6858711
0.25	1.12E+08	85282876	69791522	58869743	50444899	43596352	37834170	32866552	28505712	24623757	21129757	17956860	15054616	12384200	9915344	7624401	5493242	3509167	1667304
0.5	21276253	15876615	12799409	10659962	9029621	7719150	6628364	5697874	4889636	4177872	3544357	2975797	2462262	1996234	1572011	1185369	833440	514947.9	231490.8
0.75	6790646	4819578	3744763	3022691	2488685	2071167	1732723	1451423	1213360	1009202	832417.7	678291	543341.8	424974.5	321262.9	230829	152809.7	86953.44	34096.1
1	2583264	1729618	1287476	1002073	798236.9	643915.7	522616.4	424798.9	344484.2	277699.9	221689.1	174473.6	134599.1	100979.3	72799.26	49455.98	30529.7	15790.05	5284.258
1.5	883378	570676.9	413756.8	314919.2	245823.5	194536	154978	123664.3	98426.75	77834.56	60899.79	46916.33	35365.96	25860.87	18107.62	11884.31	7027.262	3426.848	1040.06
2	264684.9	166725	118652.3	88893.2	68401.21	53401.55	41985.88	33067.06	25972.69	20261.14	15628.77	11859.27	8794.144	6314.743	4330.922	2773.711	1590.745	743.9685	210.6409
2.5	77288.93	48090.12	33915.65	25214.53	19266.83	14942.72	11673.13	9134.933	7128.836	5524.275	4231.678	3187.335	2344.624	1668.653	1132.869	716.8725	405.0044	185.5591	50.76904
3	26555.83	16287.21	11365.57	8374.102	6346.818	4884.616	3787.383	2941.928	2278.686	1752.22	1331.443	994.2919	724.6467	510.4504	342.5192	213.769	118.7073	53.12242	13.97798
3.5	10104.21	6162.849	4283.233	3145.144	2376.435	1823.683	1410.1	1092.32	843.7291	646.9656	490.1638	364.9108	265.0642	186.0314	124.3141	77.21051	42.62019	18.92012	4.913893
4	4292.683	2655.582	1865.034	1381.697	1052.455	813.8458	633.9678	494.7348	385.0085	297.5013	227.2188	170.6123	125.0864	88.69936	59.97314	37.77035	21.21471	9.644599	2.606187
4.5	1875.781	1166.509	822.4049	611.2623	466.9826	362.1171	282.8445	221.3178	172.6987	133.8177	102.5009	77.20218	56.79024	40.41851	27.44286	17.36837	9.815206	4.49941	1.232591
5	920.8557	567.9645	397.9764	294.253	223.7235	172.6951	134.2899	104.6115	81.26179	62.67264	47.76992	35.7907	26.17712	18.51183	12.47701	7.827853	4.375206	1.97531	0.52737
5.5	540.4868	323.9549	222.2693	161.4312	120.7658	91.80592	70.33713	53.99088	41.31981	31.38348	23.54138	17.34072	12.4517	8.628063	5.682187	3.468764	1.87386	0.807593	0.19965
6	376.392	220.1154	148.3446	106.1315	78.32901	58.79535	44.49915	33.74926	25.51912	19.14575	14.18011	10.30634	7.295321	4.976569	3.220414	1.926359	1.015188	0.423456	0.099469
6.5	276.7518	158.813	105.5755	74.67242	54.54836	40.55504	30.41344	22.85966	17.13059	12.73585	9.344791	6.725849	4.711686	3.17819	2.031209	1.197868	0.620679	0.253366	0.057664
7	170.5228	95.21289	62.04848	43.15838	31.05676	22.76698	16.8438	12.49265	9.237601	6.775081	4.901837	3.476442	2.397329	1.589585	0.996657	0.574935	0.290074	0.114371	0.024689
8.5	95.09678	50.82047	32.07579	21.71683	15.25195	10.92848	7.909026	5.739789	4.152577	2.978463	2.105702	1.457442	0.97911	0.630892	0.383044	0.212856	0.102599	0.038076	0.00747
10	65.65681	34.08782	21.06634	14.01218	9.684978	6.836447	4.876678	3.489161	2.488564	1.759178	1.22512	0.834637	0.551287	0.348708	0.207373	0.112503	0.052669	0.018809	0.003475